Analytical Methods

ROYAL SOCIETY OF CHEMISTRY

PAPER

Paper-based fluorogenic RNA aptamer sensors for label-free detection of small molecules†

Cite this: DOI: 10.1039/d0ay00588f

Fatemeh Shafiei, Kathleen McAuliffe, Yousef Bagheri, Zhining Sun, Qikun Yu, Rigumula Wu* and Mingxu You *

Received 22nd March 2020
Accepted 6th May 2020

DOI: 10.1039/d0ay00588f

rsc.li/methods

Sensors based on fluorogenic RNA aptamers have emerged in recent years. These sensors have been used for *in vitro* and intracellular detection of a broad range of biological and medical targets. However, the potential application of fluorogenic RNA-based sensors for point-of-care testing is still little studied. Here, we report a paper substrate-based portable fluorogenic RNA sensor system. Target detection can be simply performed by rehydration of RNA sensor-embedded filter papers. This affordable sensor system can be used for the selective, sensitive, and rapid detection of different target analytes, such as antibiotics and cellular signaling molecules. We believe that these paper-based fluorogenic RNA sensors show great potential for point-of-care testing of a wide range of targets from small molecules, nucleic acids, proteins, to various pathogens.

Introduction

There are a growing number of diseases and health threats all around the world. Issues associated with environmental contamination and food qualities also keep increasing. Accurate, easy-to-use, and affordable point-of-care testing is highly desired.[1–4] A large number of point-of-care devices have been developed for various applications ranging from glucose testing, pregnancy testing, food pathogen detection, to disease diagnostics.[5–8] Ideal point-of-care techniques should exhibit high sensitivity and specificity, eliminating the need for lengthy tests or expensive laboratory equipment, and be easy to operate by people without special training.[9,10]

Among different probes used in point-of-care devices, nucleic acids, especially DNA aptamers, are promising candidates for the detection of various target analytes.[6,11–13] Aptamers are single-stranded DNAs or RNAs that exhibit high affinity and specificity towards their targets. For a given target, aptamers can be identified through a systematic evolution of ligands by an exponential enrichment (SELEX) process.[14,15] As a result, aptamer-based sensors can be facilely engineered for a large variety of target analytes. However, the broad applications of DNA aptamer-based point-of-care devices are still limited. This is partially because of their reduced target specificity in complex biological samples and the high cost of synthesizing dye/indicator-modified strands.[16,17]

In recent years, a type of fluorogenic RNA aptamer, such as the so-called Spinach or Broccoli, have become popular in developing biosensors.[18–21] Spinach/Broccoli can bind without a label and activate the fluorescence of dyes such as 3,5-difluoro-4-hydroxybenzylidene-1-trifluoroethyl-imidazolinone (DFHBI-1T). We and others have engineered Spinach/Broccoli into sensors for both *in vitro* and live-cell detection of metabolites, ions, proteins, and RNAs.[18,22–29] In these sensors, the target-binding RNA aptamer domain is highly selective, even in complex cellular environments. Many RNA aptamers (or riboswitches) with target-binding properties have been developed and tested through natural evolution. In addition, these fluorogenic RNA sensors can be incorporated with various genetic circuits to further improve the sensitivity and performance of the device.[23,27] As a result, we believe that these fluorogenic RNA aptamer-based sensors can be potentially useful in developing point-of-care devices with high selectivity and sensitivity.

Most of the existing fluorogenic RNA-based *in vitro* detection are performed in a sample solution using a cuvette setting. However, this setup is not user-friendly for point-of-care testing. In this study, we investigated whether these fluorogenic RNA sensors can be applied in portable devices, such as paper substrates. Naturally existing cellulose-based materials, such as paper, are popularly used substrates for point-of-care testing.[3,10,13] Paper is compatible with biological samples and can be chemically modified to incorporate different functional groups. The intrinsic porous structure of paper allows the storage of probes in the cellulose matrix. In addition, white-background paper is a good candidate for colorimetric or fluorometric tests with minimal interference in the resultant optical signal.

Department of Chemistry, University of Massachusetts, Amherst, Massachusetts 01003, USA. E-mail: rigumulawu@umass.edu; mingxuyou@umass.edu

† Electronic supplementary information (ESI) available. See DOI: 10.1039/d0ay00588f

Here, for the first time, we report the development of paper-based fluorogenic RNA aptamer devices for potential point-of-care applications. As a proof of concept, we demonstrated that these RNA-based portable devices can be used for the sensitive, selective, and accurate detection of antibiotics and signaling molecules. These paper-based devices can be stored for several months at room temperature without affecting the sensor behavior. Detection is simply performed by adding drops of the target sample onto sensor-embedded filter papers. The resulting signal can be detected within 15–30 min. We believe that these paper-based fluorogenic RNA aptamer devices can be potentially useful for point-of-care testing of various biological, medical, and daily life targets.

Materials and methods

Chemicals and reagents

All the chemicals and reagents were purchased from Sigma or Fisher unless otherwise stated and used without further purification. Guanosine tetraphosphate was purchased from Jena Bioscience (Germany). DNA oligonucleotides were synthesized and purified by Integrated DNA Technologies, Inc. or Keck Oligo Synthesis Lab at Yale University. The stock DNA oligonucleotides were dissolved at 100 μM concentration in 10 mM Tris–HCl and 0.1 mM EDTA at pH = 7.5 and stored at −20 °C. Double-stranded DNA template/non-template duplexes for *in vitro* RNA transcription were prepared by PCR amplification using an Eppendorf Mastercycler. The PCR product was further purified using a QIAquick PCR purification kit (Qiagen, Germantown, MD). The concentrations of nucleic acids were measured using a NanoDrop One UV-Vis spectrophotometer. All the RNAs for *in vitro* test were transcribed using a HiScribe™ T7 high yield RNA synthesis kit (New England BioLabs, Ipswich, MA), and then treated with RNase-free DNase I (New England BioLabs) and further purified by using a Sephadex G-25 column (GE Life Sciences). The final RNA product was verified by using 10% denaturing PAGE gels. These RNA strands were prepared into aliquots and stored at −20 °C for immediate usage or at −80 °C for long-term storage. All the RNA structures were designed using NUPACK and Mfold online software.

Solution-phase fluorescence assay

All the solution-based fluorescence measurements were conducted with a PTI fluorimeter (Horiba, New Jersey, NJ). Fluorescence assay and the assembly of RNA strands were conducted in a buffer consisting of 10 mM Tris, 5 mM $MgCl_2$, and 100 mM KCl at pH 7.5. In our measurement, fluorescence spectra in the range of 500–550 nm were collected by exciting at 480 nm.

Preparation of RNA-incorporated filter papers

Paper disks were prepared by cutting fine grade filter paper (Whatman ashless filter paper, Grade 42, 2.5 μm nominal particle retention, #1442-042) with hole punchers of different diameters. The paper disks were then autoclaved and treated with bovine serum albumin (BSA). RNA probes were mixed in folding buffer consisting of 40 mM HEPES, 100 mM KCl, 0.1% DMSO and 1 mM $MgCl_2$, at pH 7.5 and then loaded onto the prepared paper disks. Afterwards, the RNA-incorporated paper disks were flash frozen in liquid nitrogen and then dried out in a lyophilizer.

Paper-based target detection and data analysis

To detect target concentration, 8 μL of sample solution was directly added onto the above-prepared RNA-incorporated paper disks. In-paper fluorescence detection was performed with a Typhoon™ FLA 9500 biomolecular imager (GE Life Sciences). A 480 nm laser was used for excitation and the emission signal was collected at ∼520 nm, while for potential point-of-care testing, a portable UV lamp could be an option. All the data analysis was performed using ImageJ software and data plotting and fitting were accomplished by using Origin software.

Preparation of the cell lysate

Cell lysate preparation was performed following a previously reported method.[30] Briefly, 10 mL of overnight grown *E. coli* cells were treated with 1 mL of 1.9% formaldehyde solution and then incubated at 4 °C for 20 min. The cells were then precipitated by centrifugation and the supernatant was removed. Afterwards, cell pellets were resuspended in 0.5 mL of 0.1 mM KOH solution at 4 °C for 30 min. The obtained solution was neutralized with H_3PO_4 and cell debris was then separated by centrifugation. The cell lysate was finally directly added onto RNA-incorporated paper disks for target detection.

Results and discussion

Performance of Broccoli in the paper disks

First, we investigated whether fluorogenic RNAs, *e.g.*, Broccoli, could still function effectively and activate the fluorescence of DFHBI-1T in the paper substrate. Here we chose to use a fine grade Whatman® ashless filter paper, which contains >98% highly stable and polymerized α-cellulose. We expect that RNA probes can be potentially stored within these filter papers. Indeed, the function of the synthetic RNA-mediated gene network has been demonstrated in this type of paper.[13]

We chose to use Broccoli, a 49-nucleotide-long aptamer (Table S1†) that exhibits bright green fluorescence upon binding with DFHBI-1T.[18] We added 20 μM DFHBI-1T (0.16 nmol) into the filter papers (5 mm in diameter), in the presence or absence of 1 μM Broccoli (8 pmol), and then freeze-dried overnight. Afterwards, the papers were rehydrated with nuclease-free water and the fluorescence signal was detected after 30 min of incubation. Indeed, a 3.1-fold increase in the fluorescence intensity was observed in the presence of Broccoli (Fig. 1a). Broccoli RNA can still fold and bind with DFHBI-1T within the paper substrate.

Next, we investigated whether we could optimize the fluorescence intensity of the Broccoli/DFHBI-1T complex in the filter papers. It is known that bovine serum albumin (BSA), a commonly used blocking reagent, could be used to reduce the

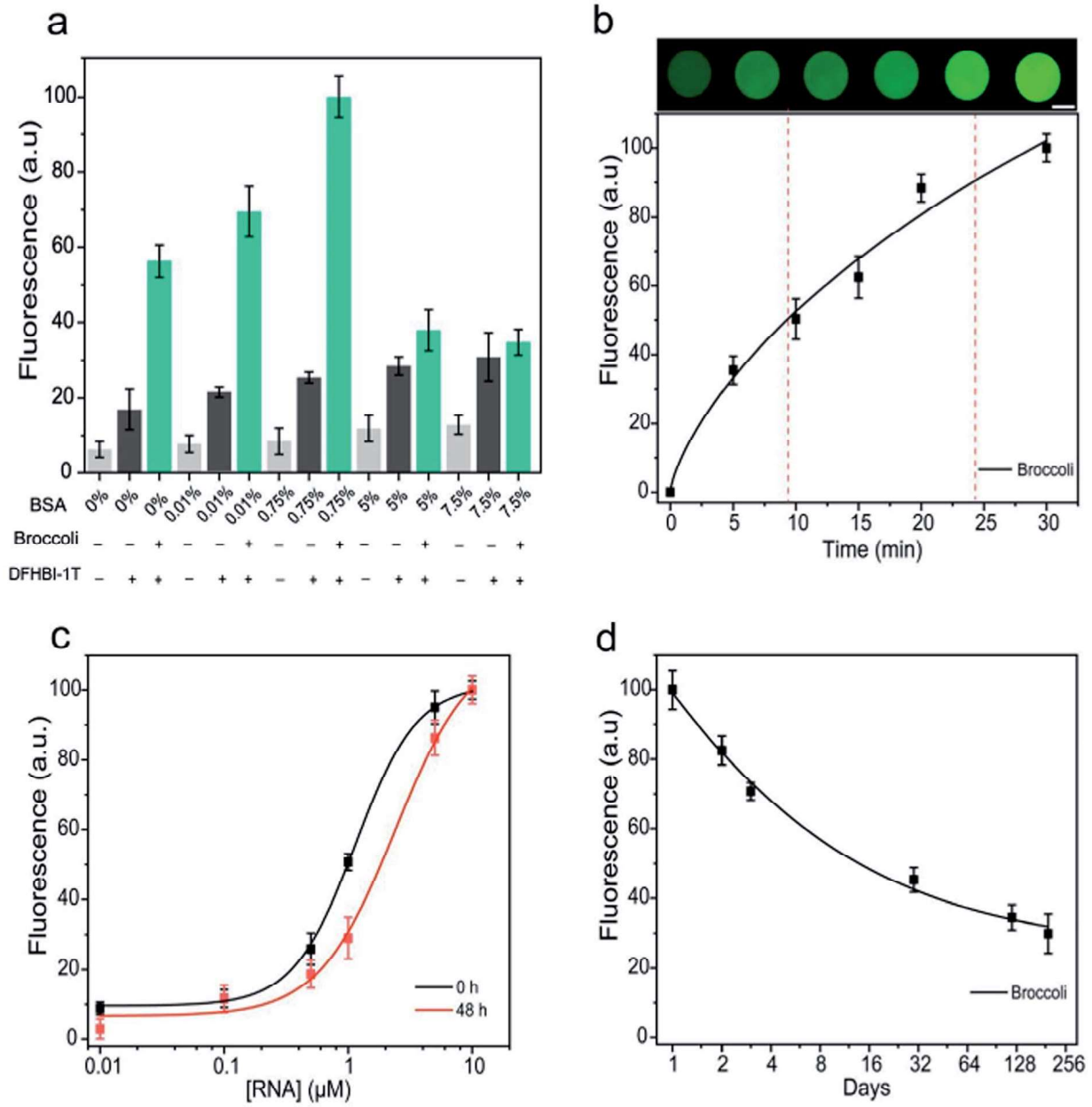

Fig. 1 Performance of Broccoli in the paper substrate. (a) Effect of BSA concentration on the Broccoli fluorescence. (b) Kinetics of Broccoli fluorescence activation in the paper. The representative images of paper-based Broccoli fluorescence after 0, 5, 10, 15, 20, and 30 min of incubation with 1 μM Broccoli RNA (8 pmol) are shown. Scale bar, 2.5 mm. (c) Detection range of Broccoli RNA in the presence of 20 μM (0.16 nmol) DFHBI-1T in either freshly prepared (0 h) or freeze-dried (48 h) paper substrates. (d) Stability of Broccoli in the freeze-dried paper substrate. The fluorescence signal was measured after different days of storage at room temperature. The mean and SD values of three independent replicates are shown.

non-specific interactions between the cellulose matrix and nucleic acids.[31,32] We wondered whether the addition of BSA will affect the folding of Broccoli and/or its binding with DFHBI-1T. To test this, we pretreated filter papers with buffers containing different percentages of BSA and then added the Broccoli/DFHBI-1T complex (Fig. 1a). Indeed, by treating with BSA, the fluorescence signal of Broccoli can be improved in the filter papers. Our result shows that 0.75% BSA-pretreated papers exhibited the largest fluorescence enhancement (5.0-fold). For the subsequent experiments, the filter papers were all pre-treated with 0.75% BSA.

Fast response kinetics are desirable for a point-of-care device. To study the fluorescence activation kinetics of Broccoli in this paper substrate, we monitored the change of the fluorescence signal immediately after mixing 1 μM Broccoli (8 pmol) with 20 μM DFHBI-1T (0.16 nmol) in the paper disks. A fast increase in the fluorescence signal was observed (Fig. 1b). It took ~9 min to reach the half-maximal fluorescence signal, and ~24 min to reach 90% of the maximal signal. Indeed, the

fluorescence signal of Broccoli can be quickly activated in the paper substrate.

We next wanted to study the correlation between the Broccoli concentration and fluorescence intensity in the paper substrate. For this purpose, 0.01–10 μM Broccoli RNA (0.08–80 pmol) was incubated with 20 μM DFHBI-1T and the corresponding fluorescence was determined. A nice sigmoid correlation was observed between the RNA concentration and the fluorescence intensity (Fig. 1c). If we defined the dynamic range as that induced 10–90% of maximum fluorescence, a moderate dynamic range was observed with 0.3–5 μM RNA. We also compared the fluorescence signal in the papers before and after the freeze-drying process. A quite similar fluorescence response was observed even after 48 h of lyophilization (Fig. 1c). The freeze-drying process did not affect the performance of Broccoli. The Broccoli fluorescence signal can be directly correlated with the RNA concentrations in the paper.

We have further determined the detection limit of this paper-based system. Our results indicated that as low as 0.2 μM (1.6 pmol) Broccoli can be detected in the paper substrate when 20 μM DFHBI-1T was used (Fig. 1c). For the paper disk with the smallest size (1.6 mm in diameter) we used, with only 0.5 μL of the sample was needed, as low as 0.1 picomole Broccoli RNA can be reliably detected (Fig. S1†). Indeed, these paper-based devices are highly sensitive and can be used for detecting a small amount of fluorogenic RNAs.

It is also important for a point-of-care device to be stable for a long period of time under normal storage conditions. To test the

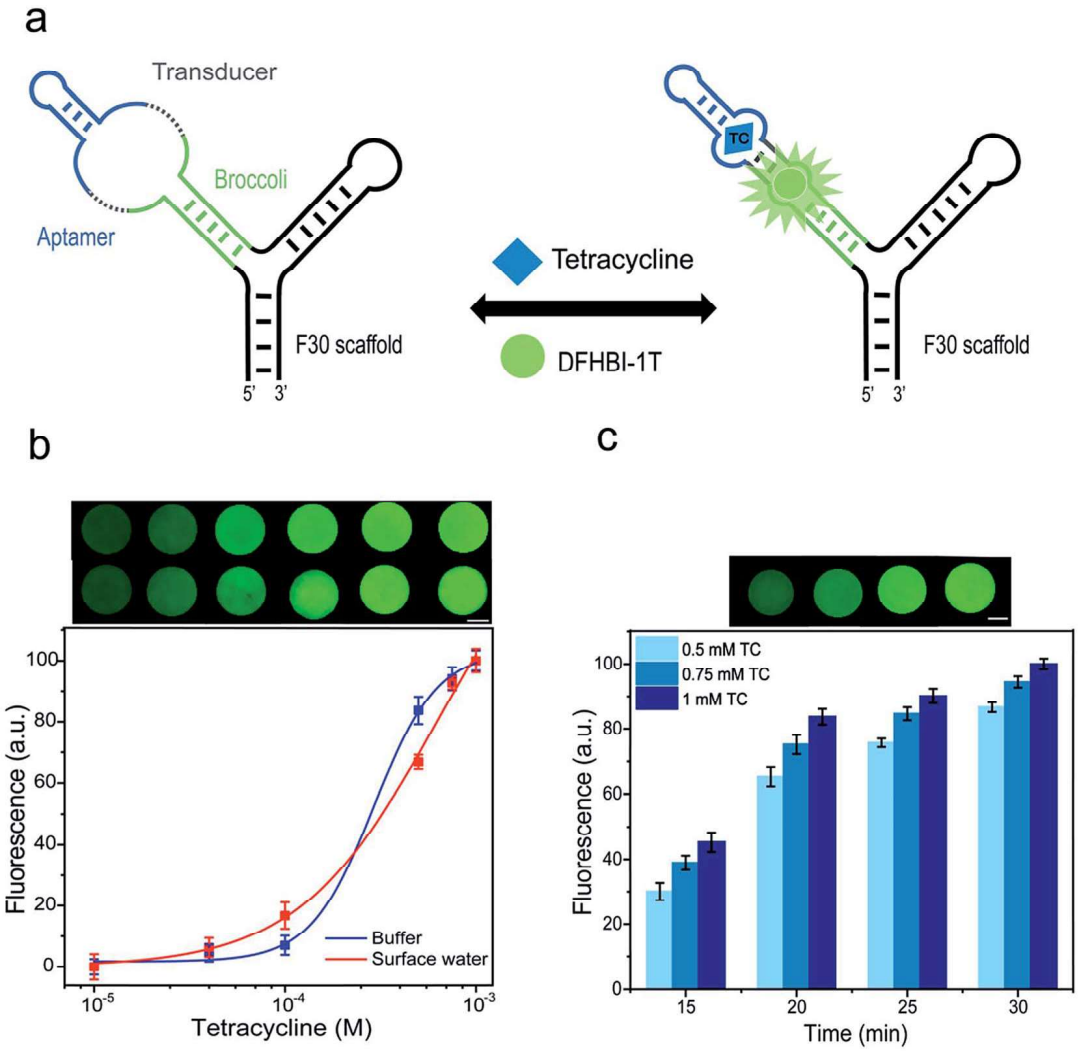

Fig. 2 Paper-based Broccoli tetracycline sensor. (a) Schematic of tetracycline-induced structural change in the sensor and fluorescence activation. The sensor platform comprises an F30 scaffold (black) and a Broccoli-based tetracycline sensor. Tetracycline binding to the aptamer (blue) stabilizes the transducer duplex (gray dashed line), enabling Broccoli (green) to fold and activate the fluorescence of DFHBI-1T. (b) Dose–response curve for the fluorescence detection of tetracycline in buffer and river water samples. The representative images of paper-based sensor fluorescence (top row, buffer; bottom row, surface water) at tetracycline concentrations of 10, 40, 100, 500, 750, and 1000 μM after 30 min of incubation are shown. (c) Kinetics of tetracycline (TC)-induced fluorescence activation in the paper substrate. The representative images of paper-based sensor fluorescence at 15, 20, 25, and 30 min after adding 750 μM tetracycline are shown. The mean and SD values of three independent replicates are shown. Scale bar, 2.5 mm.

stability of fluorogenic RNAs in the paper substrate, we first embedded 1 μM Broccoli and 20 μM DFHBI-1T into 0.75% BSA-coated papers and freeze-dried. After being stored at room temperature for different periods of time, the fluorescence signal in the paper was measured after rehydration. Broccoli was quite stable in the paper, a >50% fluorescence signal was conserved after one week of storage, and ~30% fluorescence still remained even after >200 days of storage at room temperature (Fig. 1d). We think that RNA degradation should be the major reason for the observed fluorescence decay. By adding RNase inhibitors and pretreating the paper substrate and container, the RNA degradation could be potentially further reduced.

Taken together, our results showed that Broccoli can effectively fold in the paper substrates and activate the fluorescence signal of DFHBI-1T. These fluorogenic RNA aptamers can be potentially used to develop sensors for point-of-care testing.

Paper-based Broccoli sensors for the detection of antibiotics

After optimizing the performance of Broccoli in the paper, we next investigated whether Broccoli RNA-based sensors could also function in the paper substrates. For this purpose, we first selected tetracycline as a target molecule. Tetracycline is one widely used type of antibiotic for the treatment of bacterial infections.[33] The existence and leftover of tetracycline in drinking water, agricultural and dairy products has been shown to induce bacterial antibiotic resistance.[34] It is thus important to develop point-of-care devices to rapidly detect tetracycline in these real life samples.

We and others have recently engineered a type of allosteric sensor based on fluorogenic RNA aptamers.[18–29] By fusing a target-binding aptamer with fluorogenic RNA, sensors can be developed for different analytes, including tetracycline.[26,28] Here, we engineered a Broccoli-based tetracycline sensor (Table S1†) and then applied it for the detection of tetracycline in the paper substrate. In our sensor design, the binding of tetracycline with the aptamer region induced the folding of Broccoli, which will further activate the fluorescence of DFHBI-1T and give bright green fluorescence (Fig. 2a). An F30 three-way junction RNA scaffold was further used to improve the folding and stability of the whole sensor.

To test the performance of this tetracycline sensor in the paper, 1 μM *in vitro* transcribed sensor RNA and 10 μM DFHBI-1T were embedded into the filter paper and freeze-dried overnight. After rehydration and incubation for 30 min, indeed, a 1.7-fold, 3.6-fold, and 4.3-fold increase in the fluorescence signal was observed in the presence of 100, 750, and 1000 μM tetracycline. To further study the tetracycline concentration range that these sensors could detect, a dose–response curve was generated (Fig. 2b). Under our experimental conditions, the half-maximal fluorescence was reached after adding ~250 μM tetracycline. A moderate dynamic range of tetracycline, 0.1–0.8 mM (0.8–6.4 nmol), can induce 10–90% of maximum fluorescence. Indeed, these paper-based tetracycline sensors can be potentially suitable for the detection of tetracycline in real samples.[34]

We next investigated whether these Broccoli-based tetracycline sensors could selectively recognize tetracycline over other antibiotics. We added 750 μM tetracycline, tobramycin, gentamicin, doxycycline, kanamycin, streptomycin, and ampicillin, respectively, into the sensor-embedded paper disks. As expected, the fluorescence signal was only activated in the presence of tetracycline (Fig. 3a). Indeed, these paper-based sensors can detect tetracycline with high selectivity.

We further studied the fluorescence response kinetics of the tetracycline sensor. To investigate this, we start recording the fluorescence signal immediately after adding 0.5, 0.75, and 1 mM tetracycline (Fig. 2c). The fluorescence signal in the paper can be quickly observed. Half-maximal fluorescence and 90% of

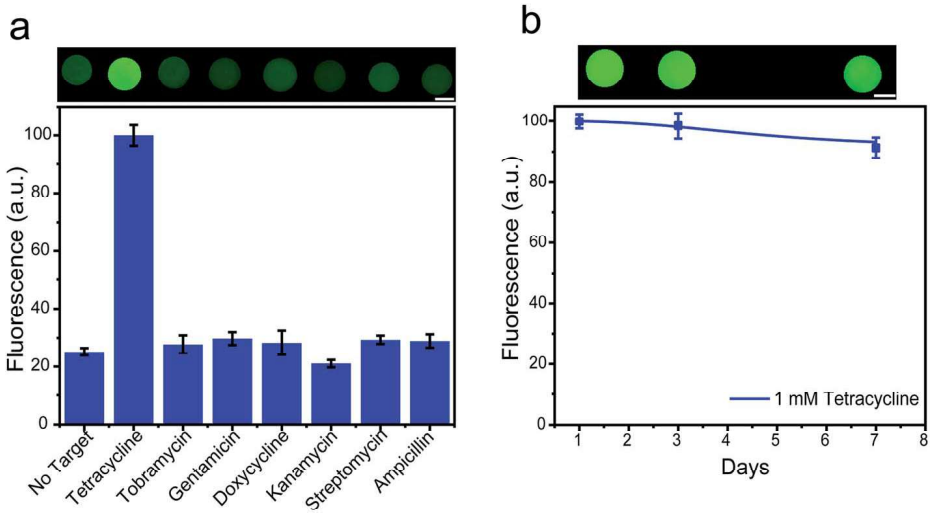

Fig. 3 Performance of the Broccoli-based tetracycline sensor. (a) Selectivity of the tetracycline sensor measured in the presence of 1 μM sensor RNA, 10 μM DFHBI-1T, and 750 μM of each antibiotic. The representative images of paper-based sensor fluorescence 30 min after adding each antibiotic are shown. (b) Stability of the tetracycline sensor measured after different days of storage at room temperature. The representative images of paper-based sensor fluorescence at each time point after adding 1 mM tetracycline are shown. The mean and SD values of three independent replicates are shown. Scale bar, 2.5 mm.

the maximal signal were reached at around 15 min and 25 min, respectively.

We also tested the stability of paper-based tetracycline sensors after week-long storage at room temperature. As shown in Fig. 3b, the sensor can still be reliably used to detect tetracycline with only 23% loss in the fluorescence signal. Indeed, the freeze-dried RNA-embedded paper device is quite stable under normal storage conditions.

All the previous tests were performed in RNase-free buffer; we next investigated whether these paper-based sensors can also function by adding a real water sample. We started with local tap water (Amherst, MA, USA). After adding different amounts of tetracycline, indeed, the paper-based tetracycline sensor exhibited quite similar tetracycline-induced fluorescence intensity in both RNase-free water and tap water (Fig. S2†).

We next tested the performance of paper-based tetracycline sensors with surface water. For this purpose, we acquired a water sample directly from the Connecticut River in the New England region of the United States. We then doped different concentrations of tetracycline into this river sample. After 30 min of incubation in the paper embedded with 1 μM RNA sensor and 10 μM DFHBI-1T, the increase in the fluorescence signal (Fig. 2b) fitted nicely with the calibration curve determined in buffer. Broccoli-based sensors indeed can be used for tetracycline detection in the river sample. There was no detectable amount of tetracycline in the tested Connecticut River sample, but it could be interesting in the future to apply this paper device to detect tetracycline concentrations in other agricultural and dairy samples.

Paper-based Broccoli sensors for the detection of signaling molecules

We wondered whether other Broccoli-based sensors could also function in the paper substrate. We chose guanosine tetraphosphate (ppGpp) as another example. PpGpp is an important signaling molecule that is produced in bacterial cells for a stringent response.[30,35,36] The generation of ppGpp helps bacteria to survive under harsh conditions by redistributing resources and regulating the expression of various enzymes and transcription factors.[36] It is critical to reliably and rapidly detect

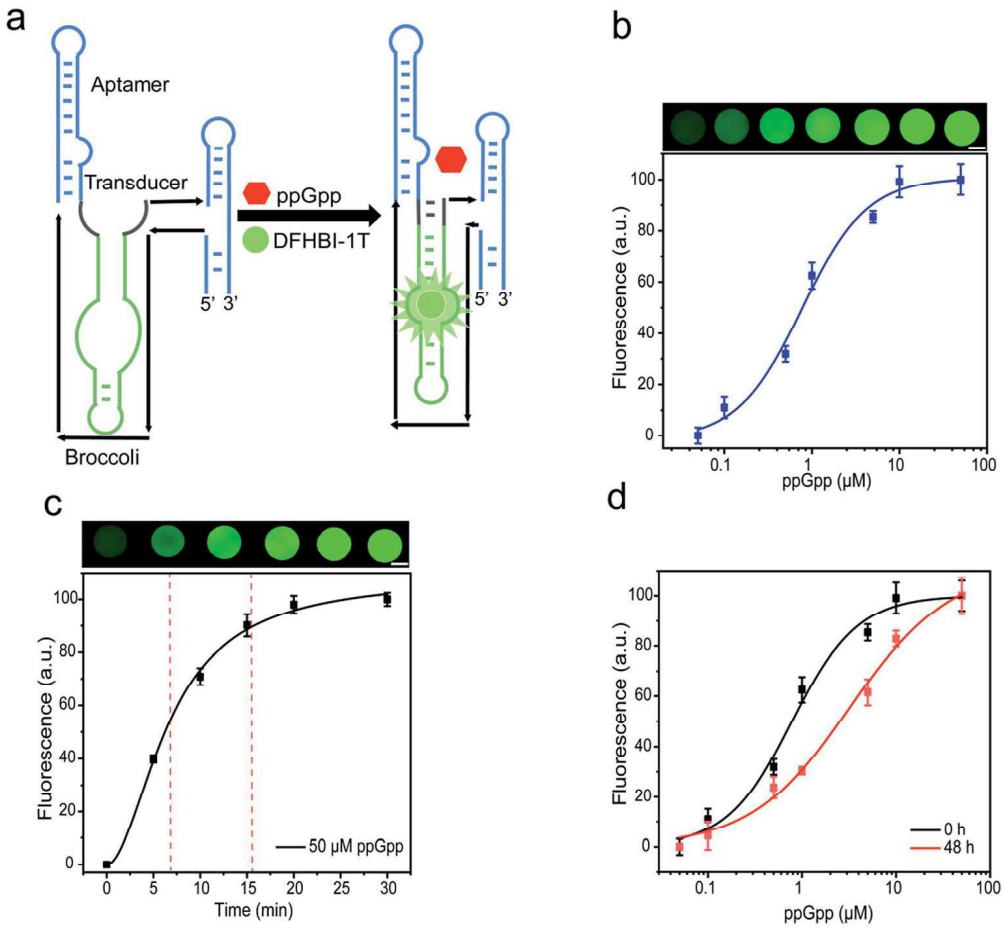

Fig. 4 Paper-based Broccoli ppGpp sensor. (a) Schematic of ppGpp-induced structural change in the sensor and fluorescence activation. (b) Dose–response curve for the fluorescence detection of ppGpp. The representative images of paper-based sensor fluorescence at ppGpp concentrations of 0.05, 0.1, 0.5, 1, 5, 10, and 50 μM after 30 min of incubation are shown. (c) Kinetics of ppGpp-induced fluorescence activation in the paper substrate. The representative images of paper-based sensor fluorescence at 0, 5, 10, 15, 20, and 30 min after adding 50 μM ppGpp are shown. (d) Detection range of the ppGpp sensor in either freshly prepared (0 h) or freeze-dried (48 h) paper substrates. The mean and SD values of three independent replicates are shown. Scale bar, 2.5 mm.

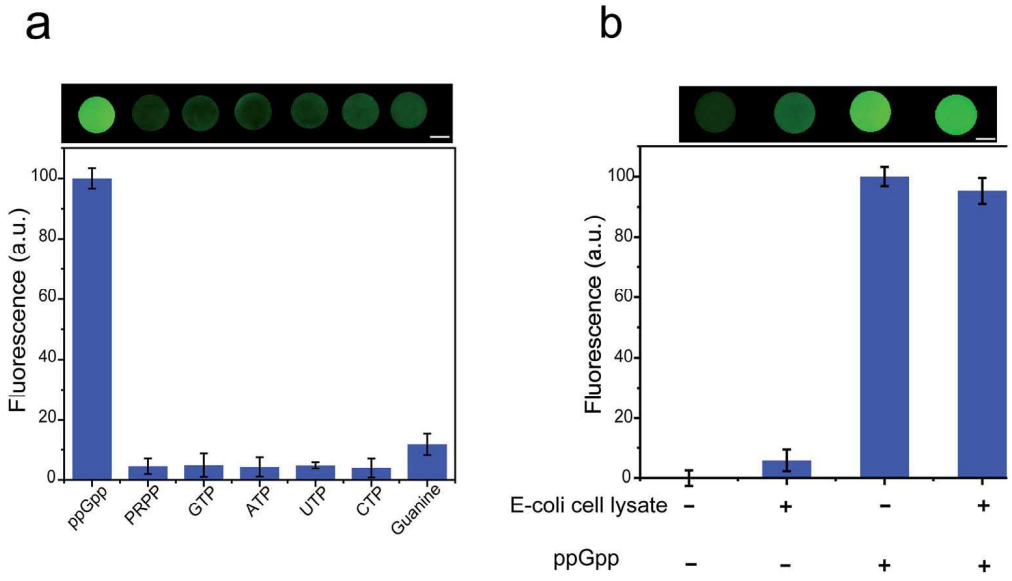

Fig. 5 Performance of the Broccoli-based ppGpp sensor. (a) Selectivity of the ppGpp sensor measured in the presence of 1 μM sensor RNA, 10 μM DFHBI-1T, and 10 μM of each indicated compound. The representative images of paper-based sensor fluorescence 30 min after adding each compound are shown. (b) Performance of the ppGpp sensor in the presence of an *E. coli* cell lysate and 1 μM ppGpp. The representative images of the corresponding paper-based sensor fluorescence are shown. The mean and SD values of three independent replicates are shown. Scale bar, 2.5 mm.

ppGpp in the cell lysate and other biological samples. The standard methods for detecting ppGpp, such as liquid chromatography and thin layer chromatography,[35,36] are time consuming, normally require radioactive labeling, and can only be performed in some specialized laboratories. Here, we aimed to develop a paper-based sensor that is easy-to-use and able to detect ppGpp with high accuracy and selectivity.

We have recently engineered a Broccoli-based probe for detecting ppGpp in solution and in living cells (unpublished results). This probe is developed based on a highly selective ppGpp-targeting RNA aptamer that was naturally evolved to bind ppGpp with high affinity.[37,38] The binding of ppGpp to the aptamer induced the folding of Broccoli and activated the fluorescence of DFHBI-1T (Fig. 4a). After incorporating 1 μM RNA sensor and 10 μM DFHBI-1T into the paper substrate and freeze-drying overnight, we added different concentrations of ppGpp. As expected, a 1.6–3.5-fold fluorescence enhancement was observed after adding 0.5–50 μM ppGpp. A moderate concentration range, 0.1–10 μM, of ppGpp (0.8–80 pmol) can be detected in this paper device (Fig. 4b). After two days of storage at room temperature, a similar 0.1–20 μM dynamic range was observed (Fig. 4d).

We also determined the sensor kinetics in the paper substrate. After adding 50 μM ppGpp, a fast fluorescence enhancement was observed, with half maximal fluorescence shown in ~7 min and 90% of maximum signal in ~15 min (Fig. 4c).

To test the selectivity of the sensor, the fluorescence intensity in the paper was measured adding 10 μM ppGpp or several other analogs. As expected, the fluorescence signal of the sensor was not activated by ppGpp analogs, including PRPP, ATP, GTP, UTP, CTP and guanine (Fig. 5a). The paper-based sensor is quite selective towards ppGpp.

Finally, we investigated whether we can use this paper-based sensor to detect ppGpp in the cell lysate. To test the performance of sensors in the cell lysate, we first lysed 8 μL of overnight grown *E. coli* cells and added different amounts of ppGpp. Based on the standard spike recovery test, 98% recovery was observed (Fig. 4b and 5b). Indeed, this paper-based sensor can be potentially used to detect ppGpp in real biological samples with a minimum operating procedure.

Conclusions

We reported here the development of fluorogenic RNA-based sensors for detecting various targets in a piece of paper. We envision that these paper-based devices could have great potential for future point-of-care applications. Paper-based artificial genetic circuits have been recently developed for the selective and sensitive point-of-care detection of various targets, including small molecules, proteins, and pathogen RNAs.[11,13,31] Enzymes and fluorescent proteins are commonly used as reporters in these genetic networks. Considering the complicated transcription and translation procedure of these circuits in generating signal readouts, fluorogenic RNA-based sensors could potentially serve as an alternative or complementary reporting system. By conjugating some of the existing genetic circuits with these fluorogenic RNAs, the sensitivity and kinetics of the system could be further improved.

In this study, for the first time, fluorogenic RNA-based sensors were incorporated into a paper substrate for future *in situ* and label-free testing. These paper-based fluorogenic RNA sensors allow us to detect target analytes in a cost-effective, selective, sensitive, and rapid manner. These sensors can be easily operated by people without professional training. For

future studies, we will test the possibility to use handheld light sources to detect these RNA-mediated fluorescence signals in paper. Considering that aptamers can be easily generated for a large variety of target analytes, we believe that this novel fluorescent sensor platform can be used to develop affordable point-of-care devices for different ions, small molecules, proteins, RNAs, and pathogens.

Conflicts of interest

The authors declare no conflict of interest.

Acknowledgements

The authors gratefully acknowledge the UMass Amherst start-up grant, NIH R01AI136789, NSF CAREER, and Alfred P. Sloan Research Fellowship to M. You. The authors also thank other members in the You Lab for useful discussion and valuable comments.

References

1 R. W. Peeling and D. Mabey, *Clin. Microbiol. Infect.*, 2010, **16**, 1062–1069.
2 D. C. Christodouleas, B. Kaur and P. Chorti, *ACS Cent. Sci.*, 2018, **4**, 1600–1616.
3 A. St John and C. P. Price, *Clin. Biochem. Rev.*, 2014, **35**, 155–167.
4 P. K. Drain, E. P. Hyle, F. Noubary, K. A. Freedberg, D. Wilson, W. R. Bishai, W. Rodriguez and I. V Bassett, *Lancet Infect. Dis.*, 2014, **14**, 239–249.
5 G. Xu, D. Nolder, J. Reboud, M. C. Oguike, D. A. van Schalkwyk, C. J. Sutherland and J. M. Cooper, *Angew. Chem., Int. Ed. Engl.*, 2016, **55**, 15250–15253.
6 M. M. Ali, M. Wolfe, K. Tram, J. Gu, C. D. M. Filipe, Y. Li and J. D. Brennan, *Angew. Chem., Int. Ed.*, 2019, **58**, 9907–9911.
7 M. N. Costa, B. Veigas, J. M. Jacob, D. S. Santos, J. Gomes, P. V Baptista, R. Martins, J. Inácio and E. Fortunato, *Nanotechnology*, 2014, **25**, 094006.
8 J. Jaeger, F. Groher, J. Stamm, D. Spiehl, J. Braun, E. Dörsam and B. Suess, *Biosensors*, 2019, **9**, 7.
9 A. M. Caliendo, D. N. Gilbert, C. C. Ginocchio, K. E. Hanson, L. May, T. C. Quinn, F. C. Tenover, D. Alland, A. J. Blaschke, R. A. Bonomo, K. C. Carroll, M. J. Ferraro, L. R. Hirschhorn, W. P. Joseph, T. Karchmer, A. T. MacIntyre, L. B. Reller and A. F. Jackson, *Clin. Infect. Dis.*, 2013, **57**, S139–S170.
10 S. Nayak, N. R. Blumenfeld, T. Laksanasopin and S. K. Sia, *Anal. Chem.*, 2017, **89**, 102–123.
11 K. Pardee, A. A. Green, M. K. Takahashi, D. Braff, G. Lambert, J. W. Lee, T. Ferrante, D. Ma, N. Donghia, M. Fan, N. M. Daringer, I. Bosch, D. M. Dudley, D. H. O'Connor, L. Gehrke and J. J. Collins, *Cell*, 2016, **165**, 1255–1266.
12 Y. Ma, G. Mao, Y. Zhong, G. Wu, W. Wu, Y. Zhan, Z. He and W. Huang, *Talanta*, 2019, **194**, 199–204.
13 K. Pardee, A. A. Green, T. Ferrante, D. E. Cameron, A. DaleyKeyser, P. Yin and J. J. Collins, *Cell*, 2014, **159**, 940–954.
14 C. Tuerk and L. Gold, *Science*, **249**, 505–510.
15 A. D. Ellington and J. W. Szostak, *Nature*, **346**, 818–822.
16 P. Kalra, A. Dhiman, W. C. Cho, J. G. Bruno and T. K. Sharma, *Front. Mol. Biosci.*, 2018, **5**, 41.
17 Q. Zhu, G. Liu, M. Kai and A. O. A. Miller, *Molecules*, 2015, **20**, 20979–90997.
18 G. S. Filonov, J. D. Moon, N. Svensen and S. R. Jaffrey, *J. Am. Chem. Soc.*, 2014, **136**, 16299–16308.
19 M. You and S. R. Jaffrey, *Annu. Rev. Biophys.*, 2015, **44**, 187–206.
20 J. S. Paige, T. Nguyen-Duc, W. Song and S. R. Jaffrey, *Science*, 2012, **335**, 1194.
21 J. S. Paige, K. Y. Wu and S. R. Jaffrey, *Science*, 2011, **333**, 642–646.
22 M. You, J. L. Litke and S. R. Jaffrey, *Proc. Natl. Acad. Sci. U. S. A.*, 2015, **112**, 2756–2765.
23 A. P. K. K. Karunanayake Mudiyanselage, Q. Yu, M. A. Leon-Duque, B. Zhao, R. Wu and M. You, *J. Am. Chem. Soc.*, 2018, **140**, 8739–8745.
24 M. You, J. L. Litke, R. Wu and S. R. Jaffrey, *Cell Chem. Biol.*, 2019, **26**, 471–481.
25 Q. Yu, J. Shi, A. P. K. K. K. Mudiyanselage, R. Wu, B. Zhao, M. Zhou and M. You, *Chem. Commun.*, 2019, **55**, 707–710.
26 R. Wu, A. P. K. K. Karunanayake Mudiyanselage, F. Shafiei, B. Zhao, Y. Bagheri, Q. Yu, K. McAuliffe, K. Ren and M. You, *Angew. Chem., Int. Ed.*, 2019, **58**, 18271–18275.
27 K. Ren, R. Wu, A. P. K. K. Karunanayake Mudiyanselage, Q. Yu, B. Zhao, Y. Xie, Y. Bagheri, Q. Tian and M. You, *J. Am. Chem. Soc.*, 2020, **9**, 11748.
28 R. Wu, A. P. K. K. Karunanayake Mudiyanselage, K. Ren, Z. Sun, Q. Tian, B. Zhao, Y. Bagheri, D. Lutati, P. Keshri and M. You, *ACS Appl. Bio Mater.*, 2020, DOI: 10.1021/acsabm.9b01237.
29 C. A. Kellenberger, S. C. Wilson, J. Sales-Lee and M. C. Hammond, *J. Am. Chem. Soc.*, 2013, **135**, 4906–4909.
30 W. A. Haseltine and R. Block, *Proc. Natl. Acad. Sci. U. S. A.*, 1973, **70**, 1564–1568.
31 K. Pardee, A. A. Green, T. Ferrante, D. E. Cameron, A. DaleyKeyser, P. Yin and J. J. Collins, *Cell*, 2014, **159**, 940–954.
32 M. Zweckstetter, G. Hummer and A. Bax, *Biophys. J.*, 2004, **86**, 3444–3460.
33 I. Chopra and M. Roberts, *Microbiol. Mol. Biol. Rev.*, 2001, **65**, 232–260.
34 C. Manyi-Loh, S. Mamphweli, E. Meyer and A. Okoh, *Molecules*, 2018, **23**, 795.
35 D. Kalia, G. Merey, S. Nakayama, Y. Zheng, J. Zhou, Y. Luo, M. Guo, B. T. Roembke and H. O. Sintim, *Chem. Soc. Rev.*, 2013, **42**, 305–341.
36 V. Hauryliuk, G. C. Atkinson, K. S. Murakami, T. Tenson and K. Gerdes, *Nat. Rev. Microbiol.*, 2015, **13**, 298–309.
37 M. E. Sherlock, N. Sudarsan and R. R. Breaker, *Proc. Natl. Acad. Sci. U. S. A.*, 2018, **115**, 6052–6057.
38 A. J. Knappenberger, C. W. Reiss and S. A. Strobel, *elife*, 2018, **7**, 36381.

